Tracking Loop Optimization for On-Board GPS Navigation in High Earth Orbit (HEO) Missions

James L Garrison, *Purdue University, West Lafayette, IN, 47907*
Michael C. Moreau, Penina Axelrad, *University of Colorado, Boulder, CO, 80309*

BIOGRAPHY

James Garrison joined the School of Aeronautics and Astronautics at Purdue University as an Assistant Professor in August of 2000. Prior to that (since 1988) he had worked for NASA, both at the Goddard Space Flight Center, in Greenbelt, MD and the Langley Research Center, in Hampton, VA. He holds a Ph.D from the University of Colorado at Boulder.

Michael Moreau is a Graduate Research Assistant at the Colorado Center for Astrodynamics Research and a Ph.D. candidate in Aerospace Engineering at the University of Colorado at Boulder. His graduate work is funded by a NASA fellowship through the Graduate Student Researchers Program at the Goddard Space Flight Center.

Penina Axelrad is Associate Professor of Aerospace Engineering Sciences at the University of Colorado, Boulder. Her research is focused on GPS technology and data analysis for aerospace applications. She has been involved in GPS-related research since 1985 and currently serves as the Chair of Satellite Division of the Institute of Navigation.

ABSTRACT

The tracking of GPS satellites in orbits which have an apogee above the GPS constellation is evaluated as a function of the code and frequency tracking loop bandwidths and predetection integration time. The distribution of the satellite carrier to noise ratio (C/N_0), acceleration, and jerk from all GPS satellites with a line of sight to the receiver antenna is computed at several different positions in the receiver orbit. Linearized models of the tracking loops are used to predict the thermal noise variance and steady state error. Requirements are also placed on the mean time to lose lock, commensurate with the duration of expected satellite passes at each orbital position. The closed loop bandwidths and integration time were determined to maximize the number of satellites tracked at different positions in the receiver orbit. Two orbits were studied: a geostationary transfer orbit and the second phase of the proposed Magnetospheric Multiscale (MMS) mission.

It was found that, as a result of the slower dynamics in these orbits, the tracking threshold could be reduced significantly by decreasing bandwidth and increasing predetection integration time when satellite visibility is poor. The need to demodulate the 50 bps data message further reduces the number satellites available. However, it is proposed to record and buffer the data message during portions of a satellite pass which are above the threshold for low bit error rates in decoding that message.

INTRODUCTION

Several future missions in NASA's Space Science Enterprise will require satellites or satellite constellations in orbits with very large eccentricities, having apogees of 10s of Earth radii. Orbit determination and relative navigation requirements for these missions are not stringent, typically in the range of 100 m or 10 % of the along-track separation between vehicles. However, there are quite severe cost constraints on these missions. For these two reasons, a strong interest exists in demonstrating the use of GPS for on-board orbit navigation as a replacement for more costly ground-based tracking. GPS has been well established for this function in Low Earth Orbit (LEO), and recent studies have indicated that it remains a viable option for many High Earth Orbit (HEO) missions when used with an orbit determination filter to sequentially process sparsely separated pseudorange measurements.

The predicted accuracy from this orbit determination is strongly dependent upon the GPS receiver tracking threshold. Previous studies have indicated that even a modest reduction of 5 to 7 dB in the threshold carrier to noise ratio (C/N_0) results in significant improvements in steady state

accuracy, through incorporation of more measurements [1]. When fewer than four satellites are visible for extended periods of time, the orbit determination accuracy is very sensitive to the clock stability. Therefore decreasing the duration of these periods (through tracking satellites at lower C/N_0) would also reduce the requirements on clock stability and thus cost.

With a tracking threshold of 30 dB-Hz, missions such as MMS could have periods of days without any measurement update. Therefore, the navigation accuracy would be very strongly dependent upon a good orbit dynamics model and a precise clock.

In the present study, ensembles of the expected C/N_0 and line of sight dynamics (acceleration and jerk) were generated for the complete GPS constellation at discrete points in the receiver orbit. A linear model was used to determine if the code and frequency tracking loop random jitter from thermal noise combined with the steady state dynamic error remained small enough for tracking to be maintained. In addition, the mean time to lose lock (MTLL) was required to be longer than the expected period of satellite visibility. This linearized model was used to determine the closed loop bandwidths of the tracking loops so as to maximize the mean number of satellites tracked for each receiver position. Thermal jitter is reduced by increased integration time and decreased bandwidth. However, steady state dynamic error follows the opposite dependence. For this reason, it was desired to provide for gain scheduling in the receiver. The closed loop bandwidth could then be changed, as a function of the estimated true anomaly of the receiver orbit.

ORBITAL SIMULATIONS

The GPS constellation was simulated using the almanac for the 27 operating GPS satellites on week 963, June 1998. The orbit/dynamics of the receiver were computed using a simple orbit propagator, which includes only the J2 oblateness term. The orbit geometry was simulated to generate time histories of the line of sight acceleration and jerk, so as to determine the steady state error in the linear models for the DLL and FLL, respectively. (Each loop was assumed to have second order closed loop transfer functions).

The GPS signal visibility model determines which GPS satellites are physically in view and transmitting signals in the direction of the receiver. L1 GPS signal Dopplers were estimated from the relative velocity of the GPS satellite projected along the line of site. Doppler rates and accelerations were computed by numerically differentiating the Doppler data. Doppler induced by oscillator errors was not modeled.

The approach taken to simulating the satellite visibility and power conditions for the HEO orbits is to evaluate, for several positions in the receiver orbit, the ensemble of line of sight dynamics, and signal power levels, for all visible GPS satellites. Visibility is determined from the conditions that the line of sight to the GPS satellite is not obscured by the Earth. The expected C/N_0 is then computed from the signal model, described in the next section.

Several discrete points in each orbit were selected corresponding to a particular altitude and true anomaly. The receiver position and velocity were held fixed and ensembles of predicted C/N_0 and line of sight dynamics (acceleration and jerk) were computed over a twelve hour period to capture a full orbital period of the GPS constellation.

Two orbits were simulated. The first was a geostationary transfer orbit (GTO) with a 26 deg. inclination based on the Inner Magnetosphere Explorer Mission (IMEX). This mission was assumed to have Earth-oriented antennas: one zenith pointing, and one nadir pointing. The second orbit had a much higher apogee. It was based on the second phase of the Magnetosphere Multiscale Mission (MMS). ($1.2 \times 30\ R_E$, 10 degree inclination) This mission was assumed to have two inertially oriented hemispherical antennas, aligned perpendicular to the ecliptic plane. The relative size of these orbits, compared to the GPS constellation is shown in figure 1.

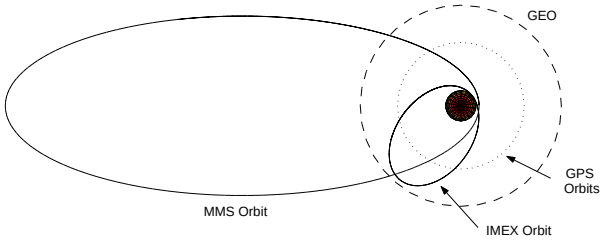

Fig. 1. Comparison of GTO, MMS and GPS Orbits

SIGNAL MODEL

C/N_0 for each visible satellite was computed using the signal model described in [2]. That model, and the assumptions used to apply it to the present study, will be briefly reviewed in this section.

The signal strength at the GPS receiver's location was modeled assuming the GPS signal transmission path illustrated in figure 2.

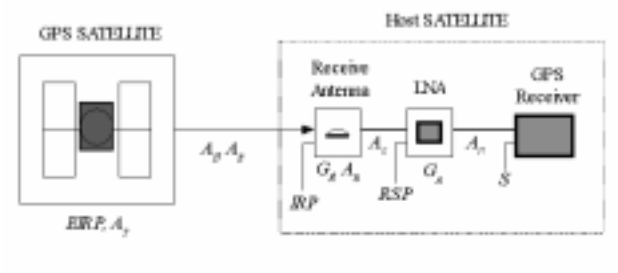

Fig. 2. GPS Signal Link Model

The isotropic received power (*IRP*), or GPS signal power at the output of the receiving antenna, is

$$IRP = EIRP + A_t + A_d + A_e$$

where $EIRP + A_t$ is the transmitted power along the line of sight direction, assuming the standard GPS SV attenuation pattern with effective isotropic radiated power ($EIRP$) of 28 dBW. A_d is the loss due to propagation of the GPS signals through space, and A_e is the loss due to transmission through the Earth's atmosphere (assumed zero except for very low altitude limb crossing signals). The carrier-to-noise spectral density at the low noise amplifier (LNA) input is computed in terms of the received signal strength by

$$C/N_0 = IRP + G_r - 10\log T_{sys} + 228.6 + A_s + L$$

where G_r is the gain of the receiving antenna in the direction of the GPS satellite, A_s is the system noise figure for the receiver (front end), L is the implementation and A/D conversion losses in the receiver, and T_{sys} is the equivalent system noise temperature.

The system noise temperature is bounded by the following two conditions, 1.) antenna pointing toward the Earth ($T_{sys} = 290K$) or 2) antenna pointed elsewhere ($T_{sys} = 180K$).

The noise figure of the receiver can be computed as follows:

$$A_s = F_1 + (F_2 - 1)/(G_a - L1) = 2.83dB$$

in which, $F_1 = 2.5dB$ (noise figure of active antenna LNA), $F_2 = 9dB$ (noise figure of MITEL GP2010 RF front end), $G_a = 26dB$ (RF gain of active antenna LNA), and $A_c = 2dB$ (loss due to RF filtering and cabling after LNA).

The GPS transmitting antennas were modeled out to an off-nadir angle of 70 degrees based on the published gain pattern for a block IIA GPS satellite [4]. Signals transmitted from off-nadir angles greater than 70 degrees were assumed to be not visible. All of the receiver antennas were assumed to be hemispherical (4.5 dB peak gain).

TRACKING LOOP MODEL

The hardware specifications of the PiVoT receiver, under development at the NASA Goddard Space Flight Center, were assumed in defining the tracking loop architecture. PiVoT utilizes four MITEL 2010 RF front-ends, and two MITEL 2021 12-channel correlator chips. Each correlator channel has a complex early and late C/A code correlator. PiVoT is based on the Compact-PCI architecture, with the front-ends and correlator chips on one Compact-PCI card, allowing selection of a separate single-card processor. A Strong-ARM processor is baselined for the flight version of the receiver. The engineering test unit uses an off the shelf Intel processor, however. Figure 3 shows the engineering model for the PiVoT RF board.

Fig. 3. PiVoT Receiver Engineering Model (courtesy of NASA Goddard Space Flight Center)

PiVoT runs the Linux operating system, in which the interfaces to the MITEL hardware, including the closed loop tracking, is incorporated into a device driver. The lower priority tasks, such as satellite selection, Doppler search, and navigation solution, are run in as user processes.

The GEONS navigation filter is incorporated as a task in the PiVoT software. GEONS is a extended Kalman filter

(EKF), using a factored covariance matrix. Spacecraft acceleration models include: JGM-2 gravity model up to degree and order 30; Earth, solar and lunar point mass gravity forces from analytical ephemerides; solar radiation pressure; and the Harris-Priester atmospheric density model. A fourth-order Runge-Kutta integrator is used. GPS pseudorange and Doppler measurements are processed to estimate a spacecraft inertial state vector.

The capability to generate pseudovelocity measurements from GEONS and use these to aide the tracking loops [3] may also be added. The present analysis, however, assumes an unaided DLL for code tracking and FLL for Doppler generation. Each of these loops uses a second order filter, with adjustable gains and predetection integration time, T_I. Lookup tables would be generated, based upon the results in this paper, for the selection of mission specific gains for the DLL and FLL.

The discriminator, and hence the closed loop transfer function, depend upon C/N_0. For this reason, a low-pass filtered measurement of the post-correlation in each channel will be monitored and used to correct the numerical values of the tracking loop gains for each satellite so as to maintain the desired bandwidth.

In the conditions of weak satellite signals, and poor visibility (ie., near apogee for an elliptical orbit) the need to maintain lock on satellites is the greatest. However, near perigee the dynamics are much less favorable, but satellite signal levels are higher. For this reason, the gain selection will be pre-determined as a function of true anomaly. This implies as a minimum, that initial satellite acquisition has been obtained. Issues related to search and initialization in an elliptical orbit will be addressed in another paper.

Three parameters will be determined, for use in these lookup tables: T_i, and the closed loop bandwidth for the DLL and FLL. These are obtained by maximizing the expected number of satellites which could be tracked. Previous work looked at the improvement of navigation accuracy as a function of tracking threshold. However, the ability of a loop to maintain track on a satellite is a function of both the signal strength and the line of sight dynamics.

Predicting if a satellite can be tracked, based upon the power level and the dynamics, is not a clearly defined problem. This is because the signal to noise ratio enters the problem through the the random thermal noise, driving the tracking loop. The condition for the loop to remain "locked" can be stated, however, in that the discriminator must generate an error signal which corrects the code delay and carrier frequency. Through linearizing this discriminator function near the tracking point, expressions for the variance of this discriminator output are commonly given as [5] [6]:

$$\sigma^2_{DLL} = \frac{B_{DLL}\,d}{2C/N_0}\left(1+\frac{2}{(2-d)C/N_0T_I}\right) \tag{1}$$

$$\sigma^2_{FLL} = \frac{1}{2\pi T_I}\frac{4B_{FLL}}{C/N_0}\left[1+\frac{1}{C/N_0T_I}\right] \tag{2}$$

for the DLL and the cross-product FLL, respectively. The discriminator variance is in units of chips^2 for the DLL, and Hz^2 for the FLL. The important parameter dependent upon the signal environment at the receiver, is C/N_0. The design parameters which can be varied include the closed-loop bandwidth, and the predetection integration time, T_i. The early-late correlator separation, d, is fixed at 0.5 chip compatible with the MITEL 2021 hardware.

It is often stated that 3 times the variance should be less than the width of the discriminator function. This assumes that the improbability of a "3 sigma" error, resulting in the loop losing lock is sufficient. These limits are as follows:

$$3\sigma_{DLL} + \frac{1}{\omega^2_{DLL}}\frac{d^2\rho}{dt^2} \le cd \tag{3}$$

$$3\sigma_{FLL} + \frac{1}{\omega^2_{FLL}}\frac{d^3\rho}{dt^3} \le c\frac{0.25}{T_I} \tag{4}$$

(For second order loops, with closed loop natural frequencies of ω_{FLL} and ω_{DLL}.) However, these limits are somewhat arbitrary, in that the true nonlinear behavior of the loops is such that it will eventually always become unstable. For this study, we considered a more conservation criterion in which these thresholds were reduced by one third through setting $c = 0.3$.

The aforementioned criteria do not always translate into the a practical determination of the loop stability. A better measure, often used, is the mean time to lose lock (MTLL). This has been computed from the nonlinear model of the DLL through integration of the Fokker-Plank stochastic differential equation. Results for the DLL have been published and numerical data from these computations, from [7], are given in figure 4.

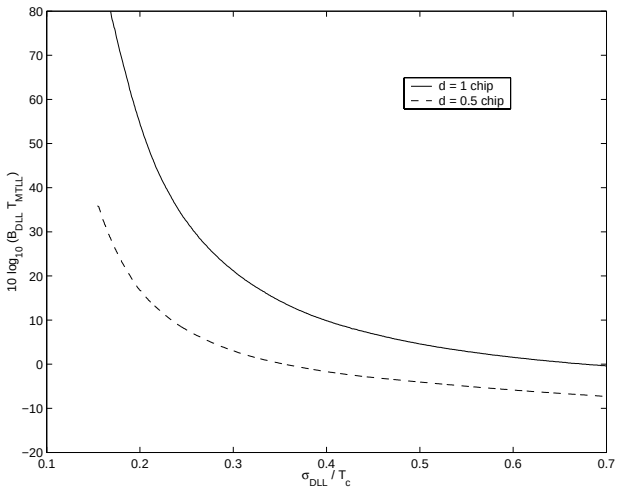

Fig. 4. DLL Mean Time to Lose Lock (from data in [7])

Using this measure, it is desired to obtain a MTLL which is greater than the expected time that a satellite would remain in view of the receiver and be used to update a position solution. Note, that for a DLL with B_L of 1 Hz, and T_I of 1 msec, the condition in (3) would result in a MTLL of about 200 seconds. An additional condition for "lock" of the DLL, in this study, is therefore that the MTLL be larger than the expected visibility of most satellites.

The following conditions were required for a satellite to be considered "tracked" at any position in the orbit: the MTLL of the DLL is larger than the maximum time of satellite visibility and that the sum of steady state error and thermal noise remain within the more conservative $c = 0.3$ threshold in equations (3) and (4).

The parameters B_L, B_{FLL} and T_I were varied to maximize the mean number of satellites which could be tracked at a given receiver orbit position. These results are to be validated in the future using a combination of Monte-Carlo simulations and hardware in the loop testing.

The aforementioned conditions only set the threshold for the loop to remain closed and within the "linear" range. A on-board position solution could not be obtained without the transmitting satellite ephemeris. The bit error rate (BER) for demodulating the data bits, is usually specified as 10^{-5}, which requires $C/N_0 = 26.5$ dB-Hz [3]. However, the ephemeris remains valid for approximately four hours, and is updated once an hour. For this reason, the satellite tracking statistics were then reevaluated for a single orbit of the receiver with the additional condition that no more than 3 hours can pass without a contact with sufficient C/N_0 to allow the ephemeris to be downloaded.

It was later concluded that this requirement on the data demodulation will be a more significant limit to the receiver's performance in low signal to noise ratio environments.

MISSION 1: GEOSTATIONARY TRANSFER ORBIT

The first example considered was the 350 by 35,700 km altitude GTO. Whereas, at apogee the visibility is such that it is often stated that between 0 and 3 satellites are visible (based upon the number of signals above conventional receiver tracking thresholds of 30 to 33 dB-Hz), the GTO case is relatively benign, and using narrower tracking loop gains near apogee significantly improves the satellite visibility.

For a geostationary satellite, the duration of the visibility for each satellite in the constellation was computed, and a histogram generated as shown in figure 5. Geostationary orbit would represent the worst case as far as duration of a pass, and hence requirements on the MTLL, is concerned, since visibility times in the remainder of the GTO will be shorter. From this figure, it can be seen that most passes (and all main lobe passes) are below 100 minutes in duration. A MTLL of 3 times this number, or 1.8×10^4 sec should be sufficient to assure tracking of all satellites for the expected duration of their passes.

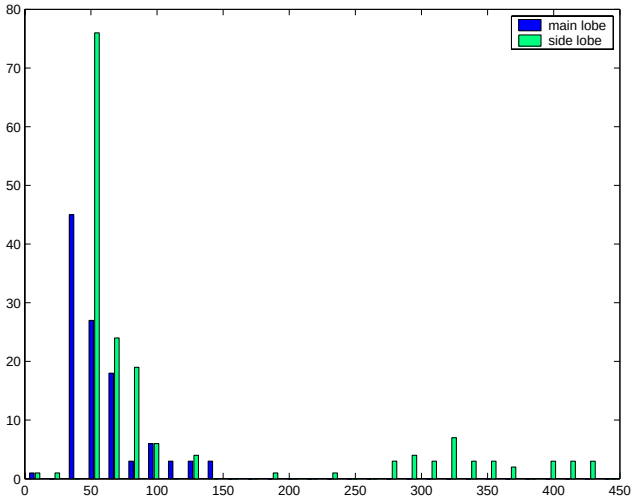

Fig. 5. Histogram of GPS Satellite Pass Durations (Geostationary Orbit)

It should also be noted that this optimization appeared to be rather "flat" in that a large variation on these values could be experienced without changing the number of expected satellites.

These results also only identify the satellites for which the DLL and FLL tracking can be maintained. As mentioned previously, there is also a requirement for demodulation of the data message. For this reason, the additional consideration was placed that a each satellite pass must be first re-

ceived at a C/N_0 high enough to decode the ephemeris before that satellite could be used in a solution. Furthermore, this ephemeris cannot be used more than 3 hours without an update.

In figure 6, a comparison of these cases in made. The first plot, uses the numerical values of B_{FLL}, B_{DLL} and T_I to maximize the expected number of available satellites. These values were computed for a receiver orbital position at perigee, perigee +15 min., perigee +45 min, and apogee. Through varying the bandwidths in this way, nearly all of the satellites, not obscured by the Earth, produce signals within the tracking threshold. The second plot shows the expected number of satellites available, under the requirement that no satellite can be used more than 3 hours since a current ephemeris was obtained. In this case, the minimum C/N_0 to demodulate the data messages was assumed to be 30 dB-Hz. The third plot of figure 6 shows a similar case, but with a reduced requirement of 26 dB-Hz to obtain the ephemeris. Finally, the fourth plot shows the expected number of satellites when using tracking loops with constant bandwidth of 1 Hz throughout the orbit.

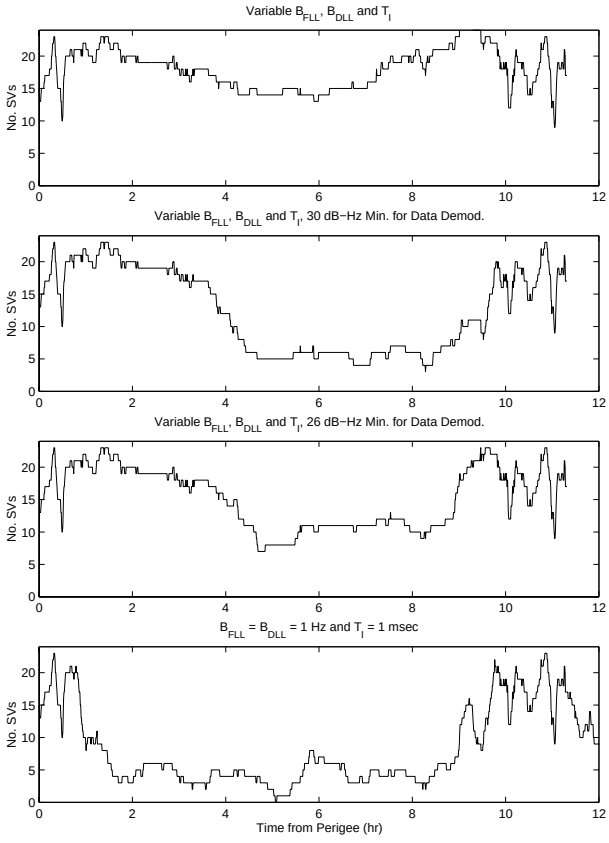

Fig. 6. Comparison of Expected Numbers of Satellites for GTO

Note first of all, through reducing the bandwidth and increasing T_I, the number of satellites for which tracking can be maintained increases significantly, in comparison to those for the $1Hz$ bandwidth case. Also, note that when the requirement for 3 hour ephemeris demodulation with the low BER is imposed, the number of satellites available for the solution is decreased significantly. It can be concluded that a primary benefit of the reduced tracking loop bandwidths is extending the duration of a satellite pass from a main lobe to a side lobe, rather than providing new satellites, with C/N_0 too low to recover the ephemeris, into the navigation solution.

MISSION 2:
MAGNETOSPHERIC MULTISCALE (MMS)

The next orbit considered is that proposed for Phase 2 of the Magnetospheric Multiscale (MMS) mission. This orbit has an apogee of 30 R_E and perigee of 1.2 R_E. At apogee, no satellites are received at C/N_0 above 29 dB-Hz. With a conventional threshold of 30 to 35 dB-Hz, the GEONS EKF would be required to propagate a solution through outages on the order of 70 hours for this 88 hour period orbit. For orbits such as this, the optimization of tracking loop bandwidth becomes more critical.

Figure 7 is a histogram of the expected duration of satellite passes at apogee for the MMS orbit. From this figure, a MTLL requirement of 3960 sec, or three times the maximum expected satellite pass, was obtained.

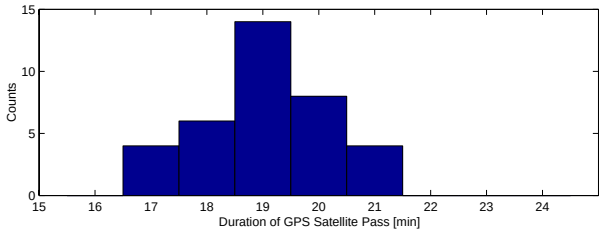

Fig. 7. Satellite Pass Duration: MMS Orbit Apogee

Through selecting the DLL and FLL bandwidths and T_I to maximize the number of satellites tracked at receiver orbital positions at perigee, perigee +40 minutes, perigee + 12 hours, and apogee, the number of satellites available for the position solution is increased throughout the orbit. These results are demonstrated in figure 8, similar to those in figure 6 for the GTO example. The first plot shows the satellites which would be available, assuming only line of sight visibility, the requirements on tracking thresholds from equations (3) and (4), and the minimum MTLL. The next two plots illustrate the requirements on data demodulation, within the previous 3 hours before generating a navigation solution, at the 30 dB-Hz and 26 dB-Hz levels. Notice, that with a 30 dB-Hz requirement on C/N_0, there remains a period of approximately 40 hours during which time no pseudoranges could be generated. Finally, the last

plot shows a comparison with the predicted results using fixed tracking loop bandwidths of 1 Hz.

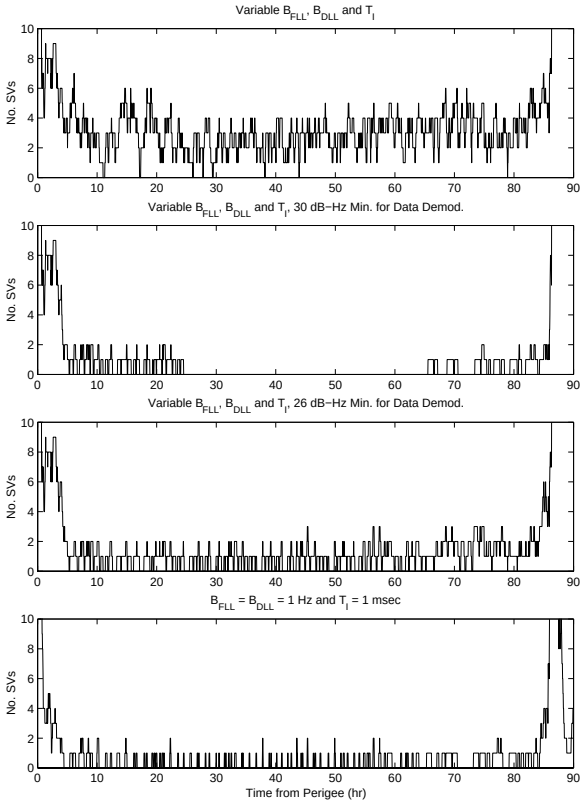

Fig. 8. Comparison of Expected Numbers of Satellites: MMS Orbit

The sensitivity of the tracking performance to the bandwidths is evaluated in table 1. Here, the FLL and DLL bandwidths are increased by a factor of 10. As this table indicates, the DLL is the most sensitive.

Table 1Sensitivity to Tracking Loop Bandwidths

B_{DLL} (Hz)	B_{FLL} (Hz)	Mean SV	>1 SV	>2 SV
0.01	0.01	2.75	87	61
0.01	0.1	2.26	76	44
0.1	0.01	0.58	11	0

The sensitivity to T_I is shown in figure 9, which plots the mean number of tracked satellites for a receiver at apogee and 12 hours past perigee. This plot indicates that similar results could be obtained with T_I less than the 20 msec maximum.

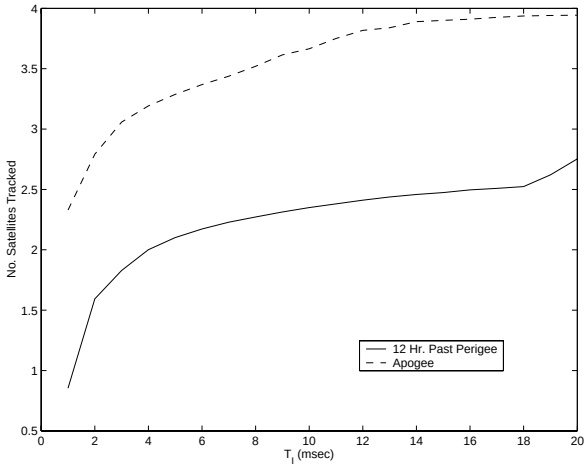

Fig. 9. Sensitivity to T_I, MMS Phase 2 Orbit

SUMMARY OF RESULTS

Figure 10 shows the closed loop bandwidths (for the FLL) obtained for the two missions described in the previous sections. The minimum bandwidth of 0.01 Hz was set because of the desire to provide the GEONS filter with independent pseudorange and Doppler measurements. The interval between measurement updates for GEONS is assumed to be between 30 seconds and 3 minutes. A bandwidth smaller than the reciprocal of this interval would produce measurements correlated in time.

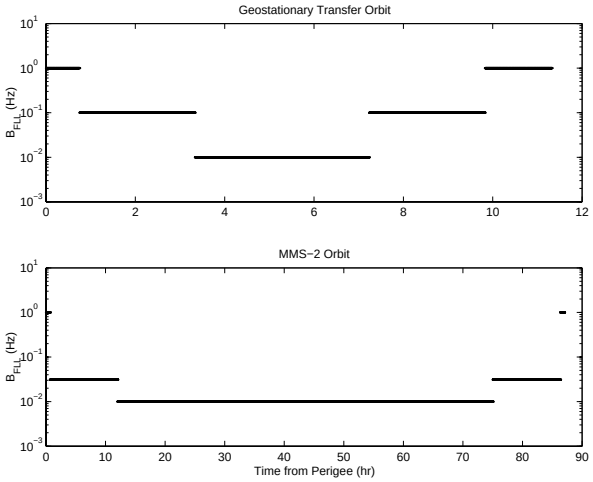

Fig. 10. Required FLL Closed Loop Bandwidth

The numbers of satellites presented in figures 6 and 8 are very optimistic. One consideration, not addressed in this study, is the uncertainty in the side lobe gain patterns of the orbiting GPS satellites. A large number of passes for the GTO example require tracking of the sidelobe. It should be noted, however, that at apogee for the MMS example, only main lobe signals are visible.

DATA DEMONDULATION

As the preceding results have indicated, the requirement to have obtained a valid satellite ephemeris at this BER, has the largest impact on reducing the available set of satellites. Several options can be considered to reduce this effect.

- Downlink pseudorange and carrier frequency data to perform portions of the orbit determination on the ground. This may not be desirable, given that one goal in the use of GPS orbit determination is to allow autonomous on-board navigation, without ground based tracking.
- Propagate broadcast ephemerides longer than the specified time. A small increase over four hours may be possible, given that the requirements on orbit determination precision, especially near apogee, is not stringent for these missions. The error growth is being investigated.
- Accumulate multiple 30 second data frames, allowing a lower BER on the individual samples.
- Store pseudorange measurements when data message can't be recovered, then "back propagate" the ephemeris, once the C/N_0 is higher. This will make the 3 hour "window" two-sided. However, real time solutions incorporating these measurements would not be possible.

CONCLUDING REMARKS

The tracking performance of the PiVoT receiver software has been predicted using several known guidelines for spread spectrum tracking loop design. Experimental validation and tuning of the receiver is expected to take place late in the summer of 2001, using the PiVoT engineering model at the GPS simulation facility at NASA Goddard Space Flight Center, Greenbelt MD. In addition, a Monte Carlo simulation of the complete receiver tracking loops under the dynamics expected in orbit is to be assembled. This would provide a design tool to allow simulation of different orbital scenarios and generate the mission specific gains for upload to the receiver.

REFERENCES

[1] M. Moreau, P. Axelrad, J. Garrison, A. Long, "GPS Receiver Architecture and Expected Performance for Autonomous Navigation in High Earth Orbits," *Navigation*, Vol. 47, No. 3, Fall 2000, pp.191-203.

[2] M. Moreau, et al, "GPS Receiver Architecture and Expected Performance for Autonomous GPS Navigation in Highly Eccentric Orbits," *55 th Annual Meeting, The Institute of Navigation*,June 28-30, 1999, Cambridge, MA.

[3] J-L Issler, et al, "High Reduction of Acquisition and Tracking Thresholds of GPS Spaceborne Receivers," ION-GPS 98, January 19, 1998.

[4] Czopek, F., "Description and Performance of the GPS Block I and II L-Band Antenna and Link Budget," *Proceedings of ION-GPS 93*, pp 37-43.

[5] Parkinson, B. W. and Spilker, J. J., eds. *Global Positioning System: Theory and Applications, Volume I*,pp. 373

[6] Natali, F. D., "AFC Tracking Algorithms," *IEEE Transactions on Communications*, Vol. 32, No. 8, August 1984, pp. 935-947.

[7] Simon, M. K., Omura, J. K., Scholtz, R. A., and Levitt, B. K., *Spread Spectrum Communications Handbook*,McGraw-Hill, 1994, pp 933.